Journal of Engineering Science and Technology
Vol. 11, No. 3 (2016) 383 - 396

REDUCTION OF NO FORMATION BY THERMAL EFFECT OF A TURBULNENT DIFFUSION FLAME H_2/AIR MODELED BY THE CONCEPT OF LAMINAR FLAMELET

HADEF AMAR[1,*], AOUACHRIA ZEROUAL[2], REZGUI YACIN[3]

[1]Department of Physics, Faculty of Science, Oum El Bouaghi University 04000, Algeria
[2]Department of Physics, Batna University 05000, Algeria
[3]Department Engineering Processes, Oum El Bouaghi University 04000, Algeria
*Corresponding Author: hadef_am@yahoo.fr

Abstract

Highly exothermic reactions are responsible for the formation of harmful polluting chemical species to humans and the biosphere. In this context, nitrogen oxides (NO_x) are pollutants that are the subject of special attention on the part of regulators. In this work we studied the impact of a co-flow swirl on the internal structure of a turbulent diffusion flame H2-N2/Air and its role in reducing the formation of NO, which is modeled by the concept of laminar flamelet, while the flow field is modeled by the standard model k-ε, with a correction term for round jets.The results show good agreement with data from the experimental data.

Keywords: Combustion, Central jet, Non-premixed flame, Laminar flamelet.

1. Introduction

At present, the pollution generated by human activities is of particular concern. It is therefore essential to work towards reducing the emission of substances potentially toxic to humans and the environment, rejected by the major recognized sources. Several countries are considering industrial use of hydrogen as fuel replacement of fossil hydrocarbons. Indeed, the gases produced by combustion do no contain CO_2, CO, soot and unburned hydrocarbons. However, the NO_x emission rates are very important [1]. The solution adopted, in general, for reducing the NO_x levels is to use premixed flames poor in hydrogen.

To avoid such risks, it is recommended to operate in diffusion flame where combustion models seized the effects of turbulent mixing on the structure of the

Nomenclatures

A	Arrhenius constant
$C_{p\ell}$	Heat capacity of species ℓ, J/kg K
$C_{\varepsilon 1}$	Coefficient model k -ε (= 1.44)
$C_{\varepsilon 2}$	Coefficient model k -ε (= 0.09)
$C_{\varepsilon 3}$	Coefficient correction Pope (= 0.50)
C_{μ}	Coefficient model k - ε (= 0.09)
D	Diffusion coefficient, m^2/s
D_h	Hydraulic diameter, m
H_{ℓ}	Specific enthalpy of species ℓ, J/kg
G_k	Production of turbulent kinetic energy, J
MW_{ℓ}	Masse molar of species ℓ ,Kg/Mol
P	Pressure, Pa
R	Ideal gas constant, J/kg.K
T	Temperature, K
u_i	Velocity in the direction i, m/s
Y_{ℓ}	Mass fraction of species ℓ
Z	Mixture fraction
Z_{st}	Stoichiometric mixture fraction

Greek Symbols

χ	Scalar dissipation rate, 1/s
ε	Dissipation rate
μ_t	Turbulent viscosity, Pa.s
$\dot{\omega}_{\ell}$	Reaction rate of species ℓ
ρ	Density, kg/m^3
σ_k	Transport coefficients k (= 1.0)
σ_E	Transport coefficients ε (=1.3)

Superscripts

~	Favre-averaged
–	Reynolds-averaged
,,	fluctuations

reaction zone of the flame, with a high strain rate in downstream of the flame due to the effect of the rapid mixing region, the turbulent transport becomes dominant over molecular diffusion which causes a perfect blend, rapid combustion and negligible time stay.

In the present study, the effects of the turbulence intensity of a co-flow with the same average speed is applied to a turbulent flame of nitrogen mixed with hydrogen diffusion, the reduction in the flame temperature is considered on the reduction of NO_x emissions in experimentally invested configuration by Hwang, et al. [2]. Reactive flow is modelled by the k-ε model with a limited correction Pope, turbulence-chemistry interaction is represented by the concept of laminar flamelet.

2. Configuration of Problem

The geometry of the problem is similar to the experimental setup invested by Hwang, C-H et al. [2] it consists of a stream of hydrogen which is derived from an injector radius R_f = 0.006 m and a mean velocity u_f of 25 m/s (Fig. 1), and another air jet with an average velocity u_a of 5m/s and radius R_a of 0.15 m (Fig. 2). For the first test, the speed fluctuations are u' = 0.19 m/s and v' = 0.07 m/s.The intensity of turbulence is about 2.50 % of the average velocity under the assumption of $v' = w'$.

For the second test, when the turbulence generator is used, the speed fluctuation increased by 3 to 7 times compared to those mentioned above, which provides values for u' = 0.52 m/s and v' = 0.50 m/s. Therefore, when the turbulence generator is used, the speed fluctuations of the air have a turbulence intensity corresponding to 10.10 % of average speed. However, the average speed of the air flow has not changed; this result shows that the turbulence generator used in this study may increase the turbulence intensity four times under the condition of an identical average speed.The turbulent kinetic energy of the air flow [3] (Fig. 3) and its dissipation rate [4] (Fig. 4) are expressed by:

$$\bar{k} = \frac{1}{2}(\bar{u}'^2 + 2\bar{v}'^2) \tag{1}$$

$$\bar{\varepsilon} = \frac{\bar{k}^{3/2}}{0.3\,D_h} \tag{2}$$

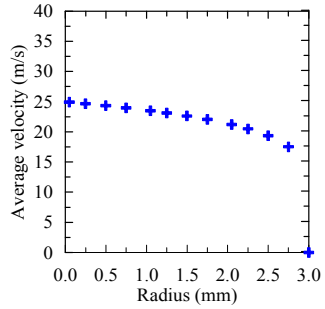

Fig. 1. Radial profiles of mean velocity of fuel.

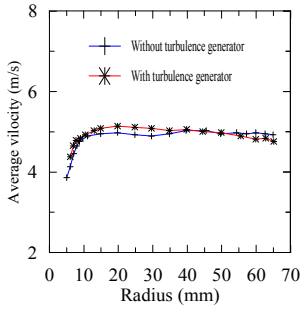

Fig. 2. Radial profiles of mean velocity of co-flow.

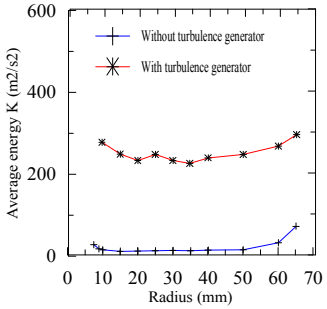

Fig. 3. Radial profiles of mean kinetic energy of co flow.

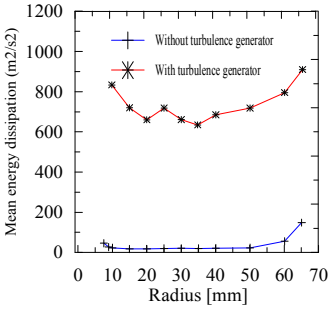

Fig. 4. Radial profile of the energy dissipation of co flow.

3. Mathematical Formulation of the Problem

3.1. Turbulence modelling

The effects of turbulence were modelled by the two-equation models of transport ($k-\varepsilon$), it is recognized that, in the configurations of the round jet and the flame of this type of jet, this model overestimates the growth rate of the jet.

It is generally possible to remedy this problem by the Pope Correction equation in the transport dissipation rate [5], which is inserted by program in C language. The flow governing equations in question are:

Mass conservation equation.

$$\frac{\partial(\overline{\rho}\,\widetilde{u}_i)}{\partial x_i}=0 \tag{3}$$

Movement equation

$$\frac{\partial(\overline{\rho}\,\widetilde{u}_j\,\widetilde{u}_i)}{\partial x_i}=-\frac{\partial\overline{P}}{\partial x_j}+\frac{\partial}{\partial x_i}\left[\mu\left(\frac{\partial\widetilde{u}_j}{\partial x_i}+\frac{\partial\widetilde{u}_i}{\partial x_j}\right)-\overline{\rho}\,\widetilde{u}_j''\,\widetilde{u}_i''\right] \tag{4}$$

Turbulence kinetic energy equation

$$\frac{\partial(\overline{\rho}\,\widetilde{u}_i\,\widetilde{k})}{\partial x_i}=\frac{\partial}{\partial x_i}\left[\left(\mu+\frac{\mu_t}{\sigma_k}\right)\frac{\partial\widetilde{k}}{\partial x_i}\right]+\overline{\rho}\,\mathrm{G}_k\text{ - }\overline{\rho}\,\widetilde{\varepsilon} \tag{5}$$

Dissipation energy equation with Pope Correction

$$\frac{\partial(\overline{\rho}\,\widetilde{u}_i\,\widetilde{\varepsilon})}{\partial x_i}=\frac{\partial}{\partial x_i}\left[\left(\mu+\frac{\mu_t}{\sigma_\varepsilon}\right)\frac{\partial\widetilde{\varepsilon}}{\partial x_i}\right]+C_{\varepsilon 1}\,\overline{\rho}\,\frac{\widetilde{\varepsilon}}{\widetilde{k}}G_k+\left(C_{\varepsilon 3}\,\widetilde{k}-C_{\varepsilon 2}\,\overline{\rho}\,\frac{\widetilde{\varepsilon}}{\widetilde{k}}\right) \tag{6}$$

with

$$\widetilde{G}_k=-\widetilde{u}_i''\widetilde{u}_j''\frac{\partial\widetilde{u}_j}{\partial x_i};\ \widetilde{u}_i''\widetilde{u}_j''=-\frac{1}{\overline{\rho}}\left[\begin{array}{l}\mu_t\left(\dfrac{\partial\widetilde{u}_j}{\partial x_i}+\dfrac{\partial\widetilde{u}_i}{\partial x_j}\right)\\ -\dfrac{2}{3}\delta_{ij}\left(\mu_t\dfrac{\partial\widetilde{u}_k}{\partial x_k}+\overline{\rho}_k\,\widetilde{k}\right)\end{array}\right]\text{ and }\mu_t=c_\mu\,\overline{\rho}\,\frac{\widetilde{k}^2}{\widetilde{\varepsilon}} \tag{7}$$

Equation of state

$$\widetilde{P}=\rho\,R\,\widetilde{T}\sum_i\frac{\widetilde{Y}_\ell}{MW_\ell} \tag{8}$$

3.2. Combustion modelling

We have adopted a configuration with two opposing jets. This geometry is very important especially in the modelling of the combustion model of the laminar

flamelets. The first stream comprises fuel, the second oxidant (Fig. 5). This geometry facilitates the study of structure of laminar flame as it allows a significant simplification of the flow equations. In this configuration the jets have impact one on to the other which makes the flow steady, also the effect of the perpendicular direction to the jet (*x*-direction in the figure) is negligible compared to the parallel (*y*-direction).

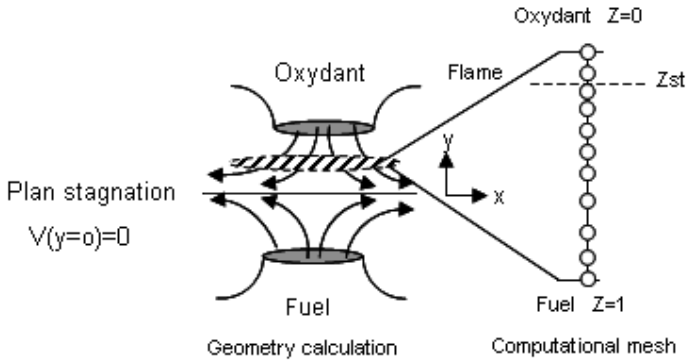

Fig. 5. Flame geometry.

The laminar flamelet structure can be determined by solving the equations of conservation of the mixture fraction, mass fractions (with a given reaction mechanism) and temperature [6]. The following assumptions are used to simplify the writing of equations:

- The Lewis number is constant Le=1.
- The Mach number is low and the density is constant.
- Adiabatic combustion (without heat loss).
- All diffusion coefficients, D_k, of chemical species are equal to D.
- The Fick's law is a good approximating the speed of diffusion.

Under these assumptions, the equation of the mixture fraction is written:

$$\frac{\partial(\rho\, Z)}{\partial \mathrm{t}} + \frac{\partial(\rho\, u_i\, Z)}{\partial x_i} = \frac{\partial}{\partial x_i}\left(\rho\, D\, \frac{\partial Z}{\partial x_i}\right) \tag{9}$$

These mass fractions:

$$\frac{\partial(\rho\, Y_\ell)}{\partial \mathrm{t}} + \frac{\partial(\rho\, u_i\, Y_\ell)}{\partial x_i} = \frac{\partial}{\partial x_i}\left(\rho\, D\, \frac{\partial Y_\ell}{\partial x_i}\right) + \dot{\omega}_\ell \tag{10}$$

and energy:

$$\frac{\partial(\rho\, T)}{\partial \mathrm{t}} + \frac{\partial(\rho\, u_i\, T)}{\partial x_i} = \frac{\partial}{\partial x_i}\left(\rho\, D\, \frac{\partial T}{\partial x_i}\right) + \frac{\dot{\omega}_\ell}{C_p} \tag{11}$$

To introduce the mixture fraction, the equations are written in the new coordinate system (Z, x_2, x_3) where the plane perpendicular to the surface of the flame is the fraction of mixture Z. The transformations of the following types Crocco [7] are applied:

$$\frac{\partial}{\partial t} = \frac{\partial}{\partial \tau} + \frac{\partial Z}{\partial t}\frac{\partial}{\partial Z} \tag{12}$$

and

$$\frac{\partial}{\partial x_1} = \frac{\partial Z}{\partial x_1}\frac{\partial}{\partial Z} \tag{13}$$

The species conservation equation gives after applying the change of reference:

$$\rho \frac{\partial Y_\ell}{\partial \tau} + Y_\ell \left[\frac{\partial \rho}{\partial t} + \frac{\partial u_i}{\partial x_i} \right] + \frac{\partial Y_\ell}{\partial Z} \left[\rho \frac{\partial Z}{\partial t} + \rho\, u_i \frac{\partial Z}{\partial x_i} - \frac{\partial}{\partial x_i}\left(\rho\, D \frac{\partial Z}{\partial x_i} \right) \right] - \rho\, D \left(\frac{\partial Z}{\partial x_i} \right)^2 \frac{\partial^2 Y_\ell}{\partial Z^2} = \dot{\omega}_\ell \tag{14}$$

The terms in brackets are zero by continuity and conservation of Z. For simplification, we can assume that:

- The normal gradient to the surface of the flame is higher than those in the tangential direction.
- The flamelet is relatively thin in the direction perpendicular to the surface of the flame.

This means that:

$$\frac{\partial^2}{\partial Z^2} >> \frac{\partial^2}{\partial \zeta_i^2} \quad (\mathrm{i} = 2,3) \tag{15}$$

Finally, one obtains:

$$\left(\frac{\partial Y_\ell}{\partial \tau} - \frac{\chi}{2}\frac{\partial^2 Y_\ell}{\partial Z^2} \right) = \frac{\dot{\omega}_\ell}{\rho \mathrm{C}_p} \tag{16}$$

with

$$\chi = 2D \left(\frac{\partial Z}{\partial x_1} \right)^2 \tag{17}$$

For the energy equation, we apply the same change with the same assumptions and we have:

$$\rho \frac{\partial T}{\partial t} = \rho \frac{\chi}{2}\frac{\partial^2 T}{\partial Z^2} - \frac{1}{C_p}\sum_\ell \dot{\omega}_\ell H_\ell + \frac{1}{2C_p}\rho\chi \left(\frac{\partial C_p}{\partial Z} + \sum_k C_{p\ell} \frac{\partial Y_\ell}{\partial Z} \right) \frac{\partial T}{\partial Z} \tag{18}$$

where H_ℓ is the specific enthalpy of species ℓ.

The scalar dissipation rate is given as a function of Z for a flame jet opposite [8]:

$$\chi(Z) = \frac{3a_s \left(\sqrt{\rho_\infty / \rho} + 1 \right)^2}{4\pi \left(2\sqrt{\rho_\infty / \rho} + 1 \right)} \exp\left[-2(erfc^{-1}(2Z))^2 \right] \tag{19}$$

where ρ_∞ the density of the oxidant stream and as the rate of the stretching in the x direction for example,

$$a_s = \frac{\partial u}{\partial x} \equiv (1/\sec) \tag{20}$$

Solving equations for this reaction mechanism provides the structure of the said diffusion flame also laminar flamelet. The equations to be solved are Eqs. (16) and (18); the independent variable is the fraction of the mixture which Z varies from 0 to 1 in the oxidant in the fuel. The rate of dissipation is a scalar parameter that varies from 0 to steady state at χ_q corresponding to the extinction of flame, remains to prescribe the molar or mass fractions of species at the entrance, the temperature and pressure jets. The solver Pre PDf of fluent solves their equations and stores them in the tables containing the profiles of temperature, mass fractions for all species based on the mixture fraction, the rate of dissipation and enthalpy using any mechanism San Diego reaction [9] which contains 25 chemical species set in 53 game reactions. For the turbulent field, a statistical approach (the probability density function) of the beta type [10], which requires the solution of the transport equation of mixture fraction Z Eq. (9), is used:

$$\frac{\partial\left(\overline{\rho}\,\widetilde{u}_i\,\widetilde{Z}\right)}{\partial x_i} = \frac{\partial}{\partial x_i}\left[\left(\mu + \frac{\mu_t}{\sigma_Z}\right)\frac{\partial \widetilde{Z}}{\partial x_i}\right] \tag{21}$$

Statistical information on the fraction of the mixture is obtained from the variance of Z by:

$$\begin{aligned}\frac{\partial}{\partial x_i}\left(\overline{\rho}\,\widetilde{u}_i\,\widetilde{Z}''^2\right) &= -\frac{\partial}{\partial x_i}\left(\overline{\rho\,u_i''\,Z''^2}\right) + \frac{\partial}{\partial x_i}\left(\overline{\rho\,D\,\frac{\partial Z''^2}{\partial x_i}}\right) \\ &+ 2\,\overline{Z''\frac{\partial}{\partial x_i}\left(\rho\,D\,\frac{\partial \widetilde{Z}}{\partial x_i}\right)} - 2\,\overline{\rho\,u_i''\,Z''}\frac{\partial \widetilde{Z}}{\partial x_i} - \overline{\rho}\,\widetilde{\chi}\end{aligned} \tag{22}$$

In this work, the rate of the scalar dissipation is modelled in the turbulent flow by the following relationship [14]:

$$\widetilde{\chi} = C_\chi \frac{\widetilde{\varepsilon}}{\widetilde{k}}\widetilde{Z}''^2 \tag{23}$$

Introducing the stretching effect of the fluctuations and the mixture fraction, the model constants σ_z, $\sigma_{z,2}$ and C_χ have the following default values: σ_z = 0.9, $\sigma_{z,2}$= 0.9 and C_χ = 2.0.

3.3. Modelling NO

A NO_x postprocessor was used to predict the formation of NO from the combustion of hydrogen. NO formation is attributed to two chemical kinetic processes, which are thermal NO_x and prompt NO_x. The thermal NO_x is formed by the oxidation of atmospheric high temperature and fast and prompt NO_x nitrogen intermediates are formed by reactions to the flame front [11]. The main reactions governing the formation of thermal NO_x from molecular nitrogen are proposed by the extended mechanism, Zeldofich [12]

$$N_2 + O \underset{k-1}{\overset{k+1}{\Leftrightarrow}} NO + N \tag{24}$$

$$N + O_2 \underset{k-2}{\overset{k+2}{\Leftrightarrow}} NO + O \tag{25}$$

A third reaction is often added:

$$N + OH \underset{k-3}{\overset{k+3}{\Leftrightarrow}} NO + H \tag{26}$$

Rate constants of reactions $k_{\pm1}$, $k_{\pm2}$ and $k_{\pm3}$ were measured experimentally by Flower et al. [14], Blauwens et al. [12] and Monat et al. [13]. They are specified by means of an Arrhenius equation of the form:

$$k = A \exp\left(\frac{\theta}{T}\right) \tag{27}$$

The net rate of NO formation via the reactions 24, 25 and 26 is calculated with the following expression:

$$\begin{aligned}\frac{d[NO]}{dt} &= k_{+1}[O][N_2] + k_{+2}[N][O_2] + k_{+3}[N][OH] \\ &\quad - k_{-1}[NO][N] - k_{-2}[NO][O] + k_{-3}[NO][H]\end{aligned} \tag{28}$$

$$\frac{d[NO]}{dt} = 2k_{+1}[O][N_2]\frac{\left(1 - \frac{k_{-1}k_{-2}[NO]^2}{k_{+1}[N_2]k_{+2}[O_2]}\right)}{\left(1 + \frac{k_{-1}[NO]}{k_{+2}[O_2] + k_{+3}[OH]}\right)} \tag{29}$$

The concentrations are expressed in mol/m³.According the quasi-stationary hypothes is for the radical N, the variation of NO concentration, as a function of time, is defined by Eq. (29), and the numerical values are presented in Table 1.

Table 1. Speed constants of reactions.

Speed constants (m^3/kg.s)	A (m^3/kg.s)	θ (K)
k_{+1}	1.8×10^8	-38 370
k_{-1}	3.8×10^7	-425
k_{+2}	1.8×10^4	-4 680
k_{-2}	3.8×10^3	-20 820
k_{+3}	7.1×10^7	-450
k_{-3}	7.1×10^8	-24 560

Finally the source term S_{NO} can be calculated by the following expression:

$$S_{NO} = M_{NO}\frac{d[NO]}{dt} \tag{30}$$

This source end is then inserted into the transport equation of NO:

$$\frac{\partial(\rho Y_{NO})}{\partial t} + \frac{\partial(\rho u_i Y_{NO})}{\partial x_i} = \frac{\partial}{\partial x_i}\left[\rho D \frac{\partial Y_{NO}}{\partial x_i}\right] + S_{NO} \tag{31}$$

where, Y_{NO} and S_{NO} are the mass fraction, the term source of NO, u_i and D are the three components of the velocity and the diffusion coefficient, respectively. To determine the rate of NO formation by the Eq. (28), in concentrations of more stable species (O_2, and N_2), it is necessary to calculate the concentration of oxygen atoms and OH free radicals.

Several methods exist to calculate the concentration of monatomic oxygen (O) [15]. A first approach considers that the rate of formation of thermal NO_x is much slower than the rate of oxidation of hydrocarbons. We can therefore consider that the thermal NO will be formed once the burning process is complete. Therefore, the formation of thermal NO can be decoupled from the main mechanism "main " of combustion. Furthermore, the rate of formation of NO may be calculated by assuming that the combustion reactions are in equilibrium.

To calculate the concentration of the monatomic oxygen (O), the improved Warnatz. [16] which involves the reactions in the third species process of dissociation-recombination of oxygen, O_2, is applied.

$$O_2 + M \Leftrightarrow O + O + M \tag{32}$$

$$[O] = 36.64 T^{-\frac{1}{2}} [O_2]^{\frac{1}{2}} \exp(\frac{-27123}{T}) \tag{33}$$

With this expression, higher concentrations of [O] are obtained, with T in Kelvin, and [O] in mol/m^3. From work of Westbrook.et al. [17] and Baulchet al. [18], the concentration of OH groups is calculated from the equation below:

$$[OH] = 2.129 \times 10^2 T^{-0.57} [O_2]^{1/2} [H_2O]^{1/2} \exp(\frac{-4595}{T}) \tag{34}$$

4. Numerical Method

Equations which describe the reactive turbulent flow are elliptical of diffusion convection type with source term. These equations are discredited into algebraic equations with the Upwind scheme. The algorithm SIPMLE is used for the speed-pressure coupling, and finally the system solution of algebraic equations is obtained using Thomas algorithm [19].

5. Results and Discussion

The radial evolution temperatures are represented in Figs. 6 and 7. In the first position, x = 60 mm, calculations give place to a larger blossoming due to strong density and speed gradient effects. Moreover, the maximum temperature is calculated with a great precision, since the adopted combustion model considers a detailed chemistry.

The effect of the turbulence intensity at the co flow entrance, proved significant behaviour of the flame. Indeed, it is noticed that a more intense turbulence at the entry slightly shorten the length of the flame. This confirms the result that a more intense turbulence involves an increase in the propagation velocity of the face of the flame and thus a less stretched flame as the position of the maximum of the static temperature represents in the first station x = 60 mm of Fig. 6, which is situated at the distance R = 6 mm with a value of 1600 K in the case without turbulence generator. On the other hand, with a turbulence generator of co flow it is situated at ray R=5 mm and T=1370 K (Fig. 7).

Furthermore, the intensity of turbulence also acts on the residence time of gas in the recirculation area by the formation and development of theeddies.This influence is also noticeable on the mixing time which is assumed very short compared with the time needed for chemical reactions (Borghi, and De Destriau Soete, 1995). Accordingly, the presence of a turbulence generator causes a decrease in temperature of the flue gas.

The radial evolutions of the species O_2 are represented on the Figs.8 and 9, it is practically consumed in the zone of flame, and reproduced in the distance *R=5* mm fig.8 (a), but with strong intensity this distance becomes *R=4* mm Fig.9 (a), then it takes its initial form at the exit.

According to Fig. 6 (without turbulence generator), and in the position x = 60 mm the maximum temperature is at R = 6 mm, and in Fig. 9 in the same position, the molar fraction of the species O_2 has a value 0.10, it is due to this that the rate of formation of NO is higher in case the position x = 60 mm, it is formed from the molecular nitrogen of the air, the reaction condition $N_2 + O \underset{k-1}{\overset{k+1}{\Leftrightarrow}} NO + N$ is limiting state of this mechanism. This reaction has high activation energy; it will be faster at higher temperatures and will take place in the flame front. On the contrary in the presence of the turbulence generator, the reduction of the formation of NO species is significant, the maximum temperature is reduced it reaches a value of 1370 K, Fig. 7. This maximum is found at R = 5 mm or with a molar fraction of the species O_2 equal to 0.05 (Fig. 9). This causes the reduction of the formation of NO passing 45 ppm (Fig. 10). To 15 ppm of (Fig.11) in the first station x = 60 mm, and a value of 30 ppm to 13 ppm at a distance of x = 180 mm injection, whereas in the last position x = 300m it goes from 15 ppm to 3 ppm.

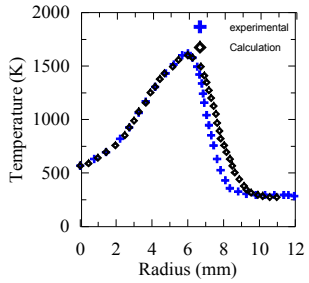

(a) Distance of the injector x = 60 mm

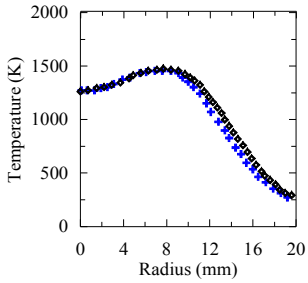

(b) Distance of the injector x = 180 mm

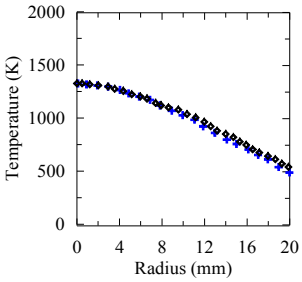

(c) Distance of the injector x = 300 mm

Fig. 6. Radial profiles of mean temperature in different sections x in the flow field (without turbulence generator).

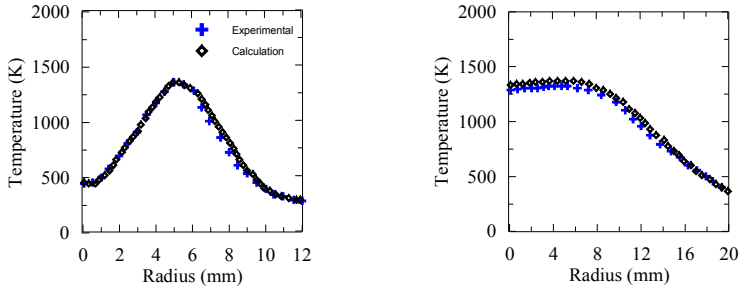

(a) Distance of the injector x = 60 mm **(b) Distance of the injector x = 180 mm**

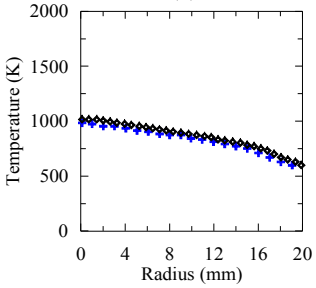

(c) Distance of the injector x = 300 mm

Fig. 7. Radial profiles of mean temperature in different sections x in the flow field (with turbulence generator).

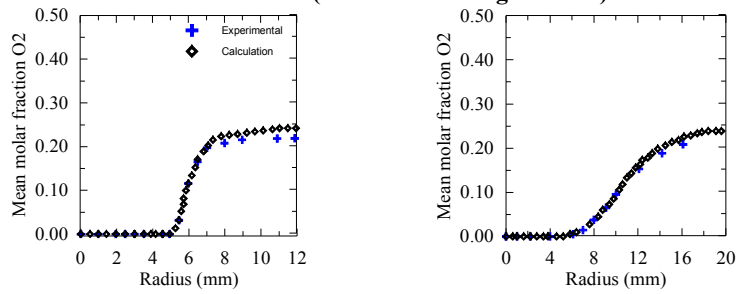

(a) Distance of the injector x = 60 mm **(b) Distance of the injector x = 180 mm**

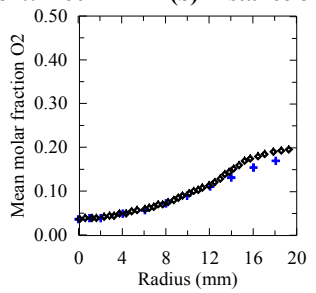

(c) Distance of the injector x = 300 mm

Fig. 8. Radial profile of the O_2 species in different sections x in the flow field (without turbulence generator).

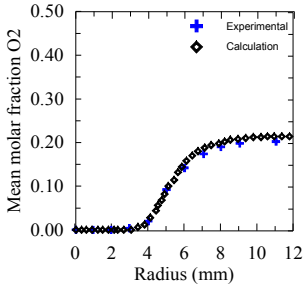

(a) Distance of the injector x = 60 mm

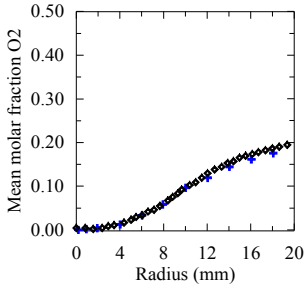

(b) Distance of the injector x = 180 mm

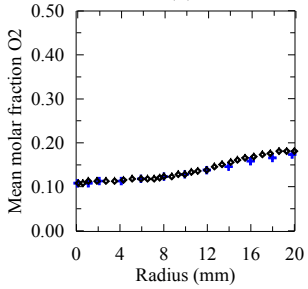

(c) Distance of the injector x = 300 mm

Fig. 9. Radial profile of the O_2 species in different sections x in the flow field (with turbulence generator).

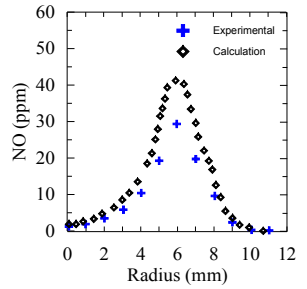

(a) Distance of the injector x = 60 mm

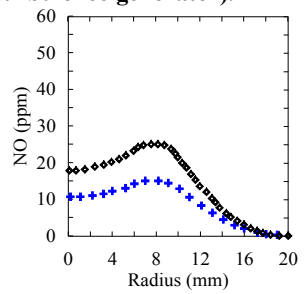

(b) Distance of the injector x = 180 mm

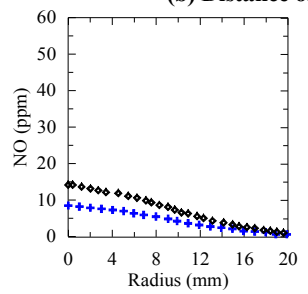

(c) Distance of the injector x = 300 mm

Fig. 10. Radial profile of the NO species in different sections x in the flow field (without turbulence generator).

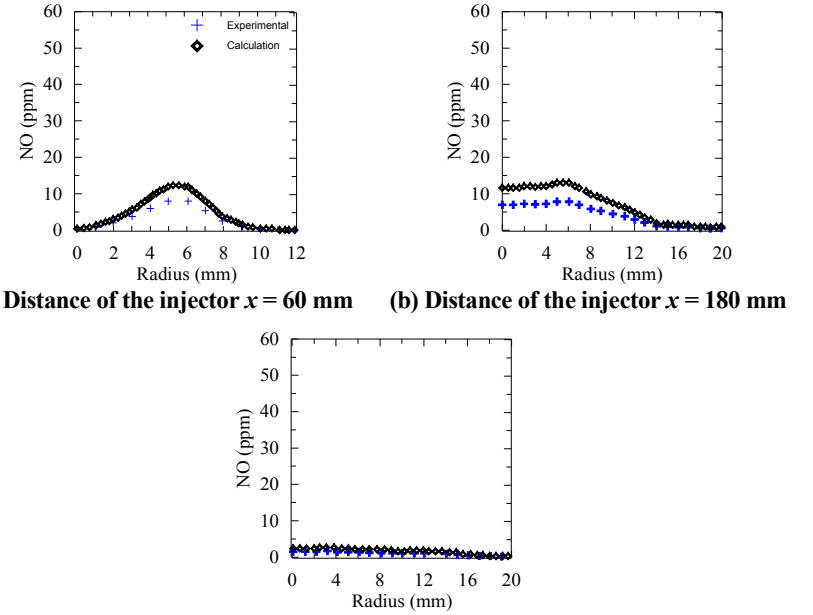

(a) Distance of the injector x = 60 mm **(b) Distance of the injector x = 180 mm**

(c) Distance of the injector x = 300 mm

Fig. 11. Radial profile of the NO species in different sections x in the flow field (with turbulence generator).

6. Conclusion

This work is to study the impact of the increased intensity of the turbulence the coflow to the internal structure of the flame, in the presence of a turbulence generator; the average width of the flame became smaller as has been demonstrated by the radial temperature profile. Any time the flame reaction zone, represented by the coexistence region of the oxygen becomes larger due to a better mixing of the resulting increase in the intensity of the turbulence reducing peak temperatures in the combustion zone. The residence time of the gases in the high temperature area and the oxygen concentration in the combustion zone, and the rate of formation of the species NO are reduced.

References

1. Inventaire des Emissions de Polluants atmospériques et de Gaz à Effet de Serre en France séries Sectorielles et Analyses Etendues (2013). Retrieved April 25,2013,from http //www.cibe.fr/IMG/pdf/secten_avril 2013_sec.pdf
2. Hwang, C.-H.; Seungro, L.; and Lee, C.-E. (2008). The effect of turbulence intensity of ambiant air flow on NO_x emissions in H_2/air non premixed jet flames. *International Journal of Hydrogen Energy*, 33(2), 832-841.
3. Schneider, C.; Dreizler, A.; Janicka, J.; and Hassel, E.P. (2003) Flow field measurements of stable and locally extinguishing hydrocarbon-fuelled jet flames. *Combustion and Flame*, 135(1-2), 185-190.

4. Mamerie, A. (2009). *Etude numérique de la combustion turbulente du prémélange pauvre méthane/air enrichi à l'hydrogéne*. Ph.D Thesis, France, Universitée d'Orléans.
5. Obieglo, A.; Gass, J.; and Poulikakos, D. (2000). Comparative study of modelling hydrogen non premixed turbulent flame. *Combustion and Flame,* 122(1), 176-194.
6. Poinsot, T.; and Veynante, D. (2005). *Theoretical and numerical combustion*. Chapter Three: Laminar diffusion flames. R.T. Edwards, 83-88.
7. Kuo, K.K.Y. (2005). Principles of Combustion. 2nd edition.
8. Peters, N. (2000). *Turbulent combustion*. Chapter Three : Non premixed turbulent combustion.Cambridge University Press, 180-185.
9. The SanDiego Mechanism (2004). Chemical-Kinetic Mechanisms for Combustion Applications, Retrieved June 10, 2013, from http://web.eng.ucsd.edu/mae/groups/combustion/mechanism.html.
10. Hadef, A.; and Aouachria, Z. (2013). The interactions of the kinetic chemistry and the turbulence on the turbulent diffusion flame. *International Conference on Mathematical Sciences and Statistics.* AIP Conference Proceedings, 1557, 174-179.
11. Konnov, A.A.; Colson, G.; and De Ruyck, J. (2001). NO formation rates for hydrogen combustion in stirred reactors. *Fuel*, 80(1), 49-65.
12. Blauwens, J.; Smets, B.; and Peeters, J. (1976) Mechanism of prompt NO formation in hydrocarbon flames. *6th symposium on Combustion*, 16(1), 1055-1064.
13. Monat, J.P.; Hanson, R.K.; and Kruger, C.H. (1979). Shock tube determination of the rate coefficient for the reaction $O + N_2 \rightarrow N + NO$. *7th Symposium on Combustion*, 17(1), 543-552.
14. Flower, W.L.; Hanson, R.K.; and Kruger, C.H. (1974). Investigation of nitric oxide decomposition in the temperature range 2500-4100 K. *5th symposium International on Combustion.* The Combustion Institute, Pittsburgh, PA. 823-832.
15. Raine, R.R.; Stone, C.R.; and Gould, J. (1995) Modelling of nitric oxide formation in spark ignition engines with a multizone burned gas. *Combustion and Flame,* 102 (3), 241-255.
16. Warnatz, J. (2001). NO_X formation in High Temperature Processes, University of Stuttgart, Germany
17. Westbrook, C.K.; and Dreyer, F.L. (1984). Chemical kinetic modelling of hydrocarbon on combustion. *Progress in Energy and Combustion Science*, 10 (1), 1-57.
18. Baulch, D.L.; Bowman, C.T.; Cobos, C.J.; Cox, R.A.; Just, Th.; Kerr, J.A.; Pilling, M.J.; Stocker, D.; Troe, J.; Tsang, W.; Walker, R.W.; and Warnatz, J. (2005). Evaluated kinetic data for combustion modelling supplement II. *Journal of Physical and Chemical Reference Data*, 34 (2), 757-1397.
19. Patankar, S.V. (1980). *Numerical Heat Transfer and Fluid Flow*, Chapter five: convection and diffusion. Hemisphere Publishing Corporation, 41977, 96-100.